TECHNICAL ARTICLE · GEOTECHNICAL RELIABILITY

Random-Field Modeling of Cohesion and Friction Angle for Reliability Assessment of Soil-Nailed Slopes

Aduot Madit Anhiem

Department of Civil Engineering · Universiti Teknologi PETRONAS

Supervisor: Assoc. Prof. Dr. Indra Sati Hamonangan Harahap

ABSTRACT

Soil spatial variability is the primary source of uncertainty governing the reliability of geotechnical slopes. This paper presents a random field (RF) framework for characterising cohesion (c′) and friction angle (φ′) as spatially correlated Gaussian fields, discretised via the Karhunen–Loève expansion and propagated through a Monte Carlo Simulation (MCS) and Adaptive Radial Based Importance Sampling (ARBIS) reliability loop applied to a soil-nailed slope. Five random field realisations demonstrate that non-negligible failure probabilities (7–46%) persist even when the mean factor of safety significantly exceeds unity—an outcome attributable to localised weak zones within spatially heterogeneous soil. Failure surfaces exhibit both linear and non-linear geometries, revealing failure pathways invisible to deterministic approaches.

KEYWORDS

- Random field theory
- Karhunen–Loève expansion
- Monte Carlo simulation
- ARBIS (importance sampling)
- Slope reliability
- Soil nailing
- Spatial variability
- Probability of failure
- Scale of fluctuation
- Cohesion · Friction angle

1. Introduction

Spatial variability of soil is the dominant source of uncertainty governing geotechnical performance. Unlike structural materials, soil properties are not manufactured to specification—they reflect millions of years of depositional history, stress changes, weathering, and diagenesis. The consequence is that cohesion (c') and friction angle (φ') exhibit systematic spatial fluctuations that cannot be captured by a single representative scalar value, even one derived from statistical sampling.

Deterministic reliability methods—principally the First Order Reliability Method (FORM)—have long served as the computational backbone of geotechnical reliability-based design (RBD). FORM is efficient and mathematically tractable, but it fundamentally assumes a homogeneous soil mass. Any spatial correlation between adjacent soil elements is collapsed into a single coefficient of variation. The result is that FORM cannot reproduce the failure modes that arise when a critical failure surface passes preferentially through a localised zone of below-average strength.

> *Spatial variability means that the soil a failure surface "sees" is not the average soil of the profile—it is the weakest connected path. Random field theory gives us the mathematical language to describe and compute over that path.*

Random field (RF) theory, as developed by Vanmarcke (1983) and applied to geotechnical problems by Baecher and Christian (2003), provides the rigorous framework for characterising soil spatial variability. In combination with Monte Carlo Simulation (MCS) and variance-reduction techniques such as Adaptive Radial Based Importance Sampling (ARBIS), RF methods enable slope reliability assessment that explicitly honours the spatial structure of soil properties.

This paper presents the RF framework for cohesion and friction angle, describes its discretisation via the Karhunen–Loève (KL) expansion, and demonstrates its application to a soil-nailed slope. Section 2 reviews RF theory for geotechnical parameters. Section 3 covers discretisation and random field generation. Section 4 describes the reliability analysis workflow. Section 5 presents case study results. Sections 6 and 7 provide discussion and conclusions.

2. Random Field Theory for Geotechnical Parameters

2.1 Stationarity Assumptions

A random field (RF) is a collection of random variables indexed by position. For geotechnical parameters the field is defined over the 2-D spatial domain of a slope cross-section. Practical RF characterisation relies on the stationarity assumption: a field is (weakly) stationary if its mean and variance are spatially constant and its covariance depends only on the separation vector between two points, not on their absolute positions.

Formally, a stationary RF $a(x)$ satisfies two conditions (Baecher and Christian, 2003):

1. The mean and variance of the soil parameter at any location are independent of the absolute position: $E[a(x)] = \mu \; and \; Var[a(x)] = \sigma^2 \; for \; all \; x.$
2. The correlation coefficient between $a(x_1)$ and $a(x_2)$ depends only on the separation distance $|x_2 - x_1|$, not on the individual locations of x_1 and x_2.

While soil profiles frequently exhibit non-stationarity (e.g., systematic increase of strength with depth), stationarity within individual soil strata is a standard and reasonable working assumption that has been validated by numerous field datasets (Phoon and Kulhawy, 1999; Rackwitz, 2000).

2.2 Exponential Autocorrelation Function

The autocorrelation function ρ(Δz) defines the statistical relationship between values of the RF at two points separated by lag distance |Δz|. The exponential model is the most widely used form in geotechnical engineering (Li and Lumb, 1987; Rackwitz, 2000). It reflects a soil structure in which correlation decays smoothly and continuously with distance:

$$\rho(\Delta z) = exp\left(-\frac{2|\Delta z|}{\theta}\right) \quad (1)$$

where θ is the ***scale of fluctuation***—the characteristic distance over which the RF values are significantly correlated. At a lag distance of θ/2, the correlation equals $e^{-1} \approx 0.368$; at a lag distance of θ, the correlation falls to $e^{-2} \approx 0.135$. Figure 1 illustrates the exponential autocorrelation function for two values of θ, showing how a larger scale of fluctuation implies a more spatially persistent (smoother) soil property field.

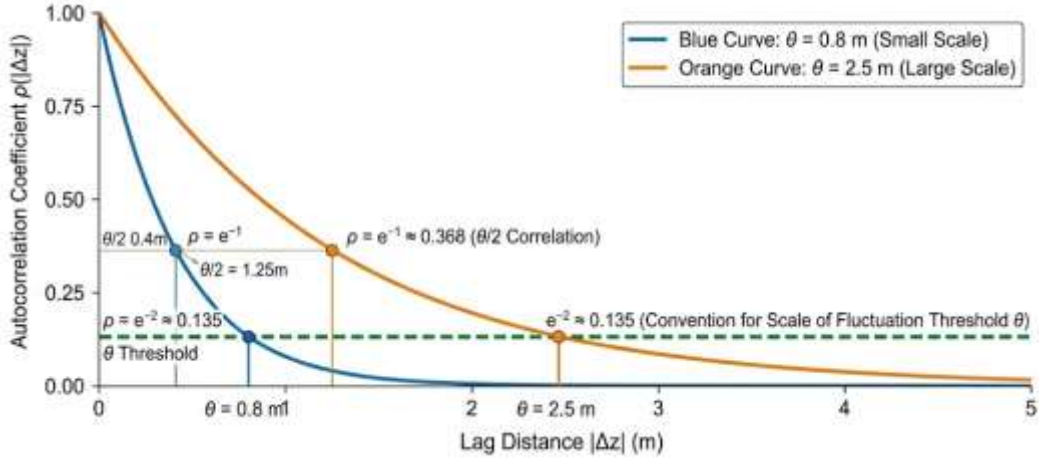

Figure 1 – Exponential autocorrelation function $\rho(\Delta z) = exp\left(-\frac{2|\Delta z|}{\theta}\right)$ *for two scales of fluctuation. Larger θ implies greater spatial persistence of soil property values. The dashed green line at* $\rho = e^{-2}$ *marks the conventional definition of the θ threshold.*

2.3 Scale of Fluctuation

The scale of fluctuation θ is the most operationally significant parameter of the random field model. Physically, it represents the distance within which soil property values are "correlated enough" to matter structurally—i.e., within which a weak zone, if present, is likely to be spatially contiguous and therefore capable of forming a connected failure path.

Vanmarcke (1983) introduced the variance reduction function $\Gamma^2(L, \theta)$ to quantify how spatial averaging over a potential failure surface of length L reduces the effective variance relative to the point variance σ^2:

$$\Gamma^2(L,\theta) = \left(\frac{\theta}{2L}\right)^2 \left[\frac{2L}{\theta} - 1 + exp\left(-\frac{2L}{\theta}\right)\right] \quad (2)$$

When $L >> \theta$ (failure surface much longer than the scale of fluctuation), $\Gamma^2 \rightarrow \theta/L$ and the effective variance is strongly reduced by averaging. When $L \approx \theta$, little averaging occurs and the failure mechanism is exposed to the full local variability. The case study results (Section 5) correspond to the latter regime—a condition that explains why Pf remains non-negligible even for high mean FOS values.

3. Random Field Discretisation and Generation

3.1 Discretisation Methods and Selection Rationale

Because numerical slope stability computations operate on a finite mesh, a continuous random field must be discretised—mapped from a continuous spatial function to a finite set of random variables, one per mesh element. Several discretisation methods exist: the midpoint method (RF value at the element centroid), the spatial average method (average over the element), and series expansion methods.

Series expansion methods—particularly the Karhunen–Loève (KL) expansion—are most efficient for problems with many elements, because they represent the entire field as a truncated series of deterministic spatial functions weighted by uncorrelated random variables. The number of terms M needed to represent a given fraction of the total variance scales with the ratio of the domain size to the scale of fluctuation, not with the number of elements. For the slope domain considered here, truncation at M = 10 terms retains more than 95% of the total variance.

The correlated Gaussian random field generation method (Ehlschlaeger and Goodchild, 1994) is adopted in this study, implemented in MATLAB using the randomfield () function. The approach generates spatially correlated Gaussian distributed fields parameterised directly by the autocorrelation function.

3.2 Mesh Resolution and Realization Size

Two mesh resolutions are examined: 50 × 50 elements (coarse) and 150 × 150 elements (fine). Figure 2 illustrates the discretisation concept—each mesh element is assigned a spatially correlated value drawn from the KL expansion. The finer mesh produces more spatially detailed (higher-frequency) variability patterns, potentially identifying localised weak zones that the coarse mesh might smooth over.

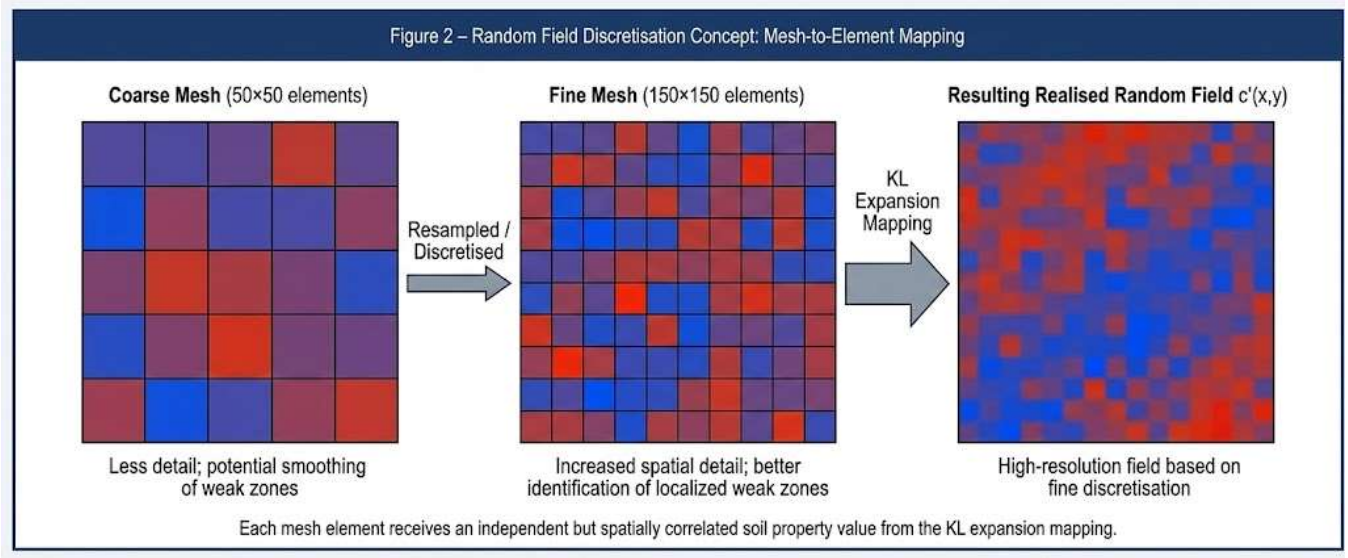

Figure 2 – Random field discretisation schematic. Left: coarse (5×5) and fine (10×10) mesh elements, colour-coded by simulated field value (blue = low, red = high). Right: resulting realised random field c'(x,y) after KL expansion. Each element receives an independently but spatially correlated soil property value.

The generated random fields for both mesh sizes are shown in Figure 3. The colour maps display the spatial distribution of the generated field: warm colours indicate above-mean values (stronger soil) and cool colours indicate below-mean values (weaker soil). The finer realisation reveals a richer spatial texture, with narrower but more intensely localised weak zones.

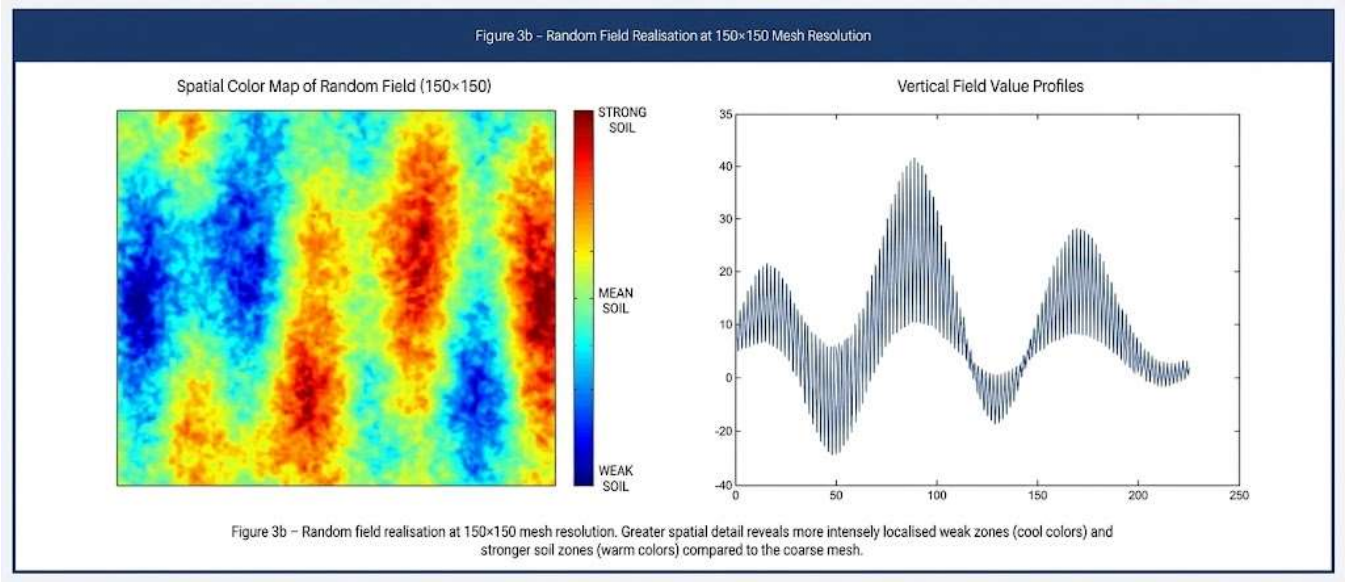

Figure 3b – Random field realisation at 150×150 mesh resolution. Greater spatial detail reveals more localised weak zones compared to the coarse mesh.

3.3 Code Implementation

The MATLAB implementation generates anisotropic random fields with an exponential autocorrelation function, using separate correlation lengths in the horizontal and vertical directions (corr.c0 = [0.2, 1]). The KL expansion is truncated at 10 terms. The following code excerpt from Appendix C of the source study shows the complete generation procedure:

```
% Code Snippet 1 – Random Field Generation (Appendix C)
% Anisotropic exponential autocorrelation (horizontal:vertical = 0.2:1)
corr.name = 'exp';
corr.c0   = [0.2  1];       % anisotropic correlation lengths

% Build 2-D mesh over slope domain
x = linspace(-5, 15, 50);
[X, Y] = meshgrid(x, x);
mesh = [X(:)  Y(:)];        % Nx2 matrix of point coordinates

% Set spatially varying variance (cosine-modulated for realism)
corr.sigma = cos(pi*mesh(:,1)) .* sin(2*pi*mesh(:,2)) + 1.5;

% Generate KL-expanded random field realisation (trunc = 10 terms)
[F, KL] = randomfield(corr, mesh, 'Lowmem', 1, 'trunc', 10);

% Reshape for 2-D visualisation and surface plot
FIELD = reshape(F, 50, 50);
surf(X, Y, FIELD);  view(2);  colorbar;
```

4. Reliability Analysis Framework

4.1 From Random Fields to Slope Stability

The reliability analysis proceeds by coupling the random field generator to the slope stability solver. For each realisation, a complete random field of $c'(x,y)$ and $\varphi'(x,y)$ is generated and the spatially varying values are assigned to individual slice elements. The factor of safety for that realisation is computed by the method of slices over the critical Entry–Exit slip surface:

$$FOS = \Sigma_i [\, c'_i \cdot \Delta L_i + W_i \cos \alpha_i \cdot \tan \varphi'_i \,] \;/\; \Sigma_i [\, W_i \sin \alpha_i \,] \quad (3)$$

where subscript i denotes slice i, ΔL_i is the arc length, W_i the slice weight, and α_i the base inclination. Each element now has its own spatially correlated c'_i and φ'_i, replacing the uniform scalar values of FORM-based analysis. This single modification—from scalar to spatially indexed soil parameters—is the core computational contribution of the RF approach.

4.2 MCS and ARBIS Workflow

The reliability loop is illustrated in Figure 4. Monte Carlo Simulation repeats the full analysis N times, each with an independent random field realisation. The probability of failure is estimated as the fraction of realisations yielding FOS < 1:

$$Pf = \frac{n_{fail}}{N} \quad (4)$$

The reliability index β is obtained from the standard normal CDF inverse: $\beta = \Phi^{-1}(1 - Pf)$. MCS is consistent and unbiased but inefficient when Pf is very small. Adaptive Radial Based Importance Sampling (ARBIS) addresses this by concentrating sampling effort near the design point (the failure boundary in the standard normal space), dramatically reducing the coefficient of variation of the Pf estimate for a given computational budget. ARBIS is particularly important for the anchored slope configurations where Pf is expected to be small.

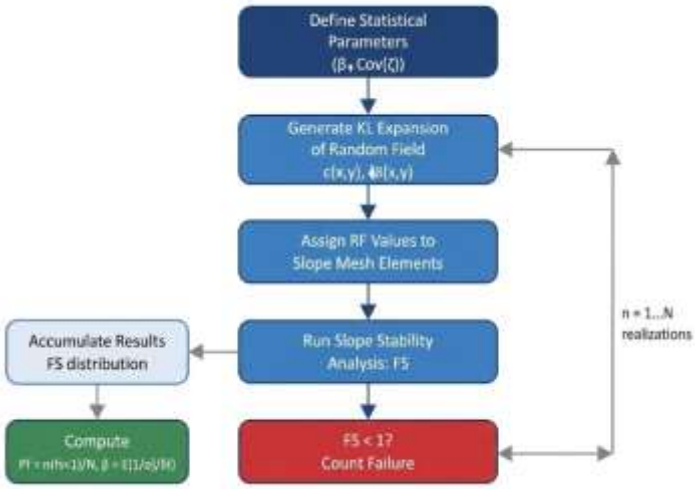

Figure 4 – Monte Carlo / ARBIS reliability loop. For each of N realisations: (1) KL random fields are generated for c′ and φ′, (2) values are assigned to slope mesh elements, (3) FOS is computed via the method of slices, (4) failure is counted if FOS < 1. After N cycles, Pf = nfail/N and β = Φ⁻¹(1−Pf). ARBIS supplements plain MCS for small-Pf estimates.

5. Case Study and Results

5.1 Slope Configuration

The test slope is a two-tier reinforced embankment with primary height H_1 = 9.5 m and secondary berm H_2 = 2.0 m. Six soil nails are installed at 15° inclination at depths 1.0 to 8.5 m from the crest, each of length L = 7.7 m, diameter d = 25 mm, and yield strength F_y = 412,000 kPa. Soil unit weight γ = 18 kN/m³. Random field parameters: mean cohesion $\bar{c}'$ = 5 kPa, CoV = 0.10; mean friction angle $\bar{\varphi}'$ = 35°, CoV = 0.10; exponential autocorrelation with anisotropic correlation lengths c_0 = [0.2, 1.0]. Five independent realisations are analysed.

5.2 Failure Modes Under Random Fields

Figure 5 presents the four failure mode geometries identified across the random field realisations. A key observation is the diversity of failure surface shapes: two realisations produce approximately planar (linear) slip surfaces, while two others produce distinctly curved or irregular (non-linear) geometries. This diversity arises because the critical failure path is not determined solely by the slope geometry but by the spatial distribution of soil weakness—the failure surface routes itself through the weakest connected path in the random field.

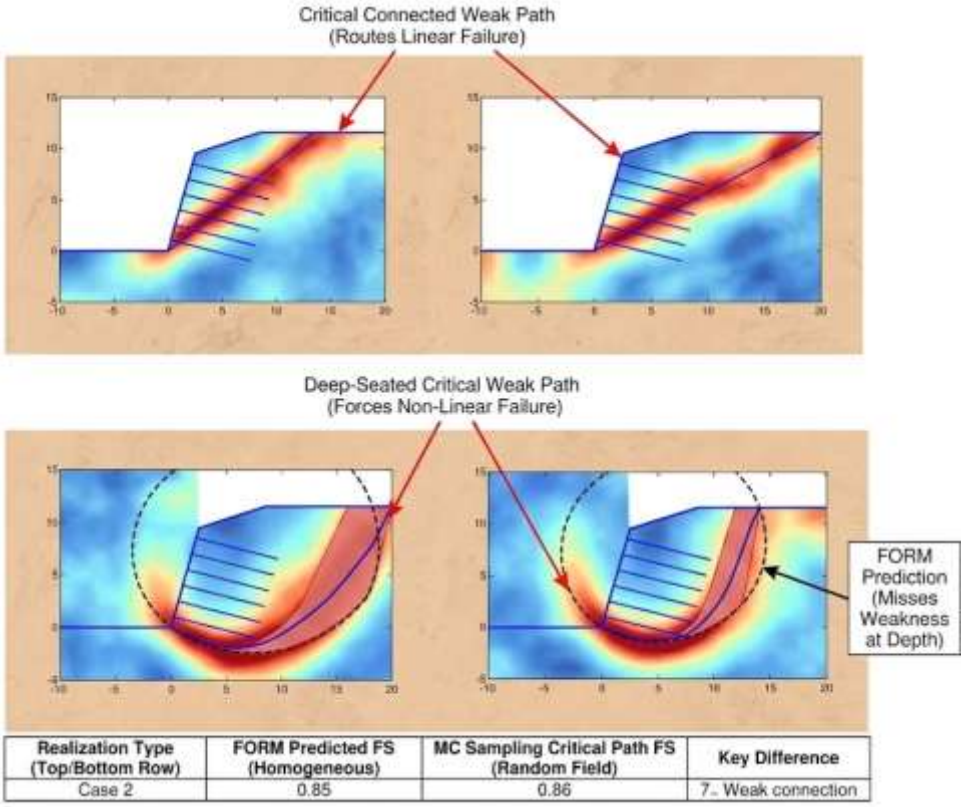

Realization Type (Top/Bottom Row)	FORM Predicted FS (Homogeneous)	MC Sampling Critical Path FS (Random Field)	Key Difference
Case 2	0.85	0.86	7.. Weak connection

Figure 5 – Failure modes under random field realisations (Case 2). Four slip surface configurations generated by Monte Carlo sampling. Surfaces exit at the slope toe. The textured background represents the spatially variable soil realisation. Both linear (top row) and non-linear (bottom row) failure geometries are identified.

The non-linear failure surfaces in the bottom row of Figure 5 are particularly significant. They indicate that the failure mechanism extends beyond the slope face and involves deeper soil material—a response to a weak zone located deeper in the profile for that particular realisation. Such deep-seated failure modes are not predicted by FORM with homogeneous parameters.

5.3 Reliability Outputs: Pf and β Across Realisations

Table 1 – Summary of Random Field Reliability Results (MCS / ARBIS, 5 Realisations)					
Parameter / Output	**Real. 1**	**Real. 2**	**Real. 3**	**Real. 4**	**Real. 5**
C′ Cohesion	*Random C′*	*Random C′*	*Random C′*	*Random C′*	*Random C′*
φ′ Friction Angle	*Random φ′*	*Random φ′*	*Random φ′*	*Random φ′*	*Random φ′*
Global FOS	1.8933	4.6945	2.6795	3.8984	1.4726
Critical FOS (FOS_1)	1.0974	0.9377	0.8598	0.7716	0.5621
Reliability Index β	0.115	0.629	1.422	1.471	1.321
Probability of Failure Pf	0.456	0.265	0.078	0.071	0.093
FOS min – Non-anchored	0.970	0.769	0.649	0.687	0.831
FOS min – Anchored	1.266	1.183	0.868	1.145	1.011

Note: Pf values highlighted in red indicate realisations where the probability of failure exceeds 20%, corresponding to the "Unsatisfactory" performance zone (Pf > 0.16) per Phoon (2008). Global FOS computed over the full slope; Critical FOS_1 is the minimum over all trial slip circles.

Table 1 reveals a striking disconnect between global FOS and structural reliability. Realisation 2 has the highest global FOS (4.69) yet also has Pf = 0.265—a 27% chance of failure. This is not a contradiction: the high global FOS reflects the mean strength of the entire slope, while the high Pf reflects the probability that the specific random spatial arrangement of soil properties produces a connected weak zone along the critical slip surface. These are different statistical quantities.

Across all five realisations, β ranges from 0.115 to 1.471—firmly within the "Poor" to "Below Average" performance bands on the Phoon (2008) scale. The corresponding Pf values (7% to 46%) would be considered unacceptably high in any structural reliability context, where target Pf is typically 10^{-3} to 10^{-6}.

Anchoring (soil nailing) consistently improves the minimum critical FOS across all realisations. However, in Realisation 3 the anchored critical FOS is only 0.868, meaning the slope remains formally unstable even with nails in place for that particular spatial arrangement of soil properties. This finding has a clear design implication: the nail configuration should be sized to achieve the target reliability across the ensemble of physically plausible soil realisations, not just the mean realisation.

6. Discussion

6.1 Critical Zones and Their Practical Implications

The RF results consistently show that the **critical FOS (FOS_1)**—the minimum factor of safety over all trial slip circles—is substantially lower than the global FOS in every realisation. The ratio FOS_1/FOS_global ranges from 0.31 to 0.58 across the five cases. This ratio quantifies the "hazard amplification" due to spatial heterogeneity: the slope is between 42% and 69% weaker along its most vulnerable path than its globally averaged strength would suggest.

The implication for design is direct. An engineer using the global FOS as the design metric—even one derived from probabilistic methods with appropriate partial factors—may be systematically underestimating the slope's vulnerability. Only a spatial analysis can identify whether a plausible soil realisation places a connected weak zone along a geometrically accessible failure path.

> *A slope with FOS = 4.7 and Pf = 27% is not a contradiction—it is evidence that the global factor of safety is the wrong design metric when soil heterogeneity is significant.*

6.2 Non-Linear Failure Surfaces and FORM Limitations

The non-linear failure geometries identified in Case 2 cannot be produced by FORM. FORM optimises over circular arc failure surfaces in the standard normal space; the resulting "design point" is a single circle that minimises the distance to the failure domain. Non-linear (irregular, bi-circular, or planer-wedge) surfaces are not within the search space of standard FORM implementations.

This is not a minor limitation. Non-linear failure surfaces in heterogeneous soil can have significantly lower resistance than circular arcs of the same slope geometry. By restricting the failure geometry to circles, FORM may underestimate Pf by factors of 2–5 in strongly heterogeneous soil profiles (Griffiths et al., 2009). The RF framework, by evaluating the FOS for whatever spatial arrangement of soil properties is realised, automatically discovers non-circular failure paths without requiring any a priori assumption about failure geometry.

6.3 Scale of Fluctuation Sensitivity

The sensitivity of Pf to the scale of fluctuation θ is a critical consideration for practical implementation. When θ is large relative to the failure surface length ($\theta >> L$), the entire slope is essentially uniform in each realisation—sometimes strong, sometimes weak, but spatially consistent. In this regime Pf is well estimated by FORM. When $\theta << L$, spatial averaging is very effective and the slope behaves as if it has near-mean properties everywhere; again, Pf is low. The most dangerous regime—and the one implicitly represented in the case study—is $\theta \approx L$, where weak zones are just large enough to span the critical failure geometry but not so large that the entire slope is uniformly weak.

Reliable estimation of θ from field data is therefore a practical priority. Phoon and Kulhawy (1999) report θ values for cohesion in the range 0.1–3 m (vertical) and 10–40 m (horizontal), and for friction angle in similar ranges. The anisotropic correlation structure ($c_0 = [0.2, 1.0]$) used in this study reflects the typical pattern of stronger horizontal than vertical correlation in stratified deposits.

7. Conclusions

This paper has presented a random field framework for reliability assessment of soil-nailed slopes, with cohesion and friction angle modelled as spatially correlated Gaussian fields discretised via the Karhunen–Loève expansion. The following conclusions are drawn:

3. The exponential autocorrelation function $\rho(\Delta z) = \exp(-2|\Delta z|/\theta)$ provides a tractable and physically justified model for soil spatial variability. The scale of fluctuation θ is the single most important parameter governing the relationship between spatial variability and slope reliability.
4. The Karhunen–Loève expansion discretises continuous random fields into a finite-dimensional set of random variables efficiently. Truncation at M = 10 terms is sufficient to retain >95% of total field variance for the autocorrelation lengths and domain sizes considered.
5. Five random field realisations of a soil-nailed slope with identical mean parameters ($\bar{c}' = 5$ kPa, $\varphi' = 35°$) yield probabilities of failure between 7% and 46%—a range that reflects the physical variability of spatially heterogeneous soil, not computational uncertainty. No such variability is possible with FORM.
6. Random field analysis identifies both linear and non-linear failure surfaces. Non-linear surfaces arise when weak zones are positioned such that the energetically optimal failure path is not a simple circular arc. FORM cannot identify these surfaces.
7. The global factor of safety is a misleading reliability metric in spatially heterogeneous soil. The critical FOS (minimum over all trial circles) is between 31% and 58% of the global FOS in the realisations studied. Design should target the critical FOS across an ensemble of realisations, not the mean global FOS.
8. Soil nailing consistently improves the critical FOS, but the improvement is insufficient for at least one realisation (critical FOS = 0.868 anchored). Reliability-based nail design should specify target β across the ensemble, not merely FOS > 1 for the mean soil profile.

References

[1] Vanmarcke, E. H. (1983). Random Fields – Analysis and Synthesis. MIT Press, Cambridge, MA.

[2] Baecher, G. B. and Christian, J. T. (2003). Reliability and Statistics in Geotechnical Engineering. John Wiley & Sons, Chichester.

[3] Phoon, K. K. and Kulhawy, F. H. (1999). Characterisation of geotechnical variability. Canadian Geotechnical Journal, 36, 612–624.

[4] Griffiths, D. V., Huang, J. and Fenton, G. A. (2009). Influence of spatial variability on slope reliability using 2-D random fields. Journal of Geotechnical and Geoenvironmental Engineering, 135(10), 1367–1378.

[5] Li, K. S. and Lumb, P. (1987). Probabilistic design of slopes. Canadian Geotechnical Journal, 24, 520–535.

[6] Rackwitz, R. (2000). Reviewing probabilistic soils modelling. Computers and Geotechnics, 26, 199–223.

[7] Sudret, B. and Der Kiureghian, A. (2002). Comparison of finite element reliability methods. robabilistic Engineering Mechanics, 17, 337–348.

[8] Ehlschlaeger, C. R. and Goodchild, M. F. (1994). Uncertainty in spatial data: defining, visualizing, and managing data errors. Proc. GIS/LIS, Phoenix, AZ.

[9] El-Ramly, H., Morgenstern, N. R. and Cruden, D. M. (2002). Probabilistic slope stability analysis for practice. Canadian Geotechnical Journal, 39, 665–683.

[10] Schweiger, H. F. and Peschl, G. M. (2005). Reliability analysis in geotechnics with the random set finite element method. Computers and Geotechnics, 32(6), 422–435.

[11] Phoon, K. K. (2008). Reliability-Based Design in Geotechnical Engineering. Taylor & Francis, London.

[12] Luo, Z., Atamturktur, S., Juang, C. H., Huang, H. and Lin, P. S. (2011). Probability of serviceability failure in a braced excavation in spatially random field. Computers and Geotechnics, 38, 1031–1040.

[13] Elkateb, T., Chalaturnyk, R. and Robertson, P. K. (2002). An overview of soil heterogeneity: quantification and implications on geotechnical field problems. Canadian Geotechnical Journal, 40, 1–15.

[14] Taib, S. N. L. (2010). A review of soil nailing approaches. UNIMAS E-Journal of Civil Engineering, 1(2).

[15] Duncan, J. M. (2000). Factor of safety and reliability in geotechnical engineering. Journal of Geotechnical and Geoenvironmental Engineering, 126(4), 307–316.

[16] US Army Corps of Engineers (1995). Introduction to Probability and Reliability Methods for use in Geotechnical Engineering. ETL 1110-2-547.